

NUMERICAL AND EXPERIMENTAL EVALUATION OF LIGHT STEEL FLOOR TRUSSES UNDER UNIFORM DISTRIBUTED LOADS

AVALIAÇÃO NUMÉRICA E EXPERIMENTAL DE TRELIÇAS DE PISO EM LIGHT STEEL FRAME SOB CARGAS UNIFORMEMENTE DISTRIBUÍDAS

EVALUACIÓN NUMÉRICA Y EXPERIMENTAL DE CERCHAS DE PISO EN LIGHT STEEL FRAME SOMETIDAS A CARGAS UNIFORMEMENTE DISTRIBUIDAS

Christovam de Moraes Weidlich

M.Sc. in Structural Engineering, Pontifical Catholic University of Rio de Janeiro, Brazil

E-mail: moraes.weidlich@gmail.com

Guilherme Fleith de Medeiros

D.Sc. in Civil Engineering, University of Passo Fundo, Brazil

E-mail: guifleith@upf.br

Zacarias Martin Chamberlain Pravia

D.Sc. in Structural Engineering, University of Passo Fundo, Brazil

E-mail: zacarias.chamberlain@gmail.com

Abstract

Due to the increasing use of Steel Framing systems in Brazilian buildings, and the still limited number of studies addressing the behavior of some of their structural components under service loading, this study investigated the relationship between numerical and experimental models for light steel floor trusses subjected to uniformly distributed loads. Experimental tests were carried out on a full-scale Light Steel Framing (LSF) floor subsystem composed of three trusses, OSB panels, and a water tank used to reproduce a controlled distributed load. The water level and flow rate were monitored throughout the tests, and the vertical displacement of the central truss was measured with digital gauges. In parallel, finite element models based on three-dimensional shell and two-dimensional beam idealizations were developed in ANSYS Workbench, with and without web-connection eccentricity. The results were compared in terms of the measured service deflection. Among the investigated approaches, the two-dimensional beam model with eccentricity showed the best agreement with the measured service deflection of the tested system. Therefore, among the evaluated idealizations, this model is recommended for simplified serviceability-oriented simulations of similar LSF floor trusses.

Keywords: Light Steel Framing (LSF); Experimental Analysis; Numerical Models; Floor Beam Truss.

Resumo

Devido ao uso crescente dos sistemas Steel Framing em edificações brasileiras e ao ainda limitado número de estudos que abordam o comportamento de alguns de seus componentes estruturais sob

carregamentos de serviço, este estudo investigou a relação entre modelos numéricos e experimentais para treliças leves de piso em aço submetidas a cargas uniformemente distribuídas. Ensaio experimentais foram realizados em um subsistema de piso em Light Steel Framing (LSF) em escala real, composto por três treliças, painéis OSB e um tanque de água utilizado para reproduzir uma carga distribuída controlada. O nível de água e a vazão foram monitorados ao longo dos ensaios, e o deslocamento vertical da treliça central foi medido com relógios comparadores digitais. Paralelamente, modelos em elementos finitos baseados em idealizações tridimensionais em casca e bidimensionais em viga foram desenvolvidos no ANSYS Workbench, com e sem excentricidade nas ligações da alma. Os resultados foram comparados em termos da flecha de serviço medida. Entre as abordagens investigadas, o modelo bidimensional em viga com excentricidade apresentou a melhor concordância com a flecha de serviço medida do sistema ensaiado. Portanto, dentre as idealizações avaliadas, esse modelo é recomendado para simulações simplificadas, voltadas à verificação de serviço, de treliças leves de piso em LSF semelhantes.

Palavras-chave: Light Steel Framing (LSF); Análise Experimental; Modelos Numéricos; Treliça de Viga de Piso.

Resumen

Debido al uso creciente de los sistemas Steel Framing en edificaciones brasileñas y al aún limitado número de estudios que abordan el comportamiento de algunos de sus componentes estructurales bajo cargas de servicio, este estudio investigó la relación entre modelos numéricos y experimentales para cerchas livianas de piso de acero sometidas a cargas uniformemente distribuidas. Se realizaron ensayos experimentales en un subsistema de piso en Light Steel Framing (LSF) a escala real, compuesto por tres cerchas, paneles OSB y un tanque de agua utilizado para reproducir una carga distribuida controlada. El nivel de agua y el caudal fueron monitoreados durante los ensayos, y el desplazamiento vertical de la cercha central fue medido con relojes comparadores digitales. Paralelamente, se desarrollaron modelos de elementos finitos basados en idealizaciones tridimensionales de cascarón y bidimensionales de viga en ANSYS Workbench, con y sin excentricidad en las conexiones del alma. Los resultados se compararon en términos de la flecha de servicio medida. Entre los enfoques investigados, el modelo bidimensional de viga con excentricidad mostró la mejor concordancia con la flecha de servicio medida del sistema ensayado. Por lo tanto, entre las idealizaciones evaluadas, este modelo se recomienda para simulaciones simplificadas orientadas a la verificación en servicio de cerchas livianas de piso en LSF similares.

Palabras clave: Light Steel Framing (LSF); Análisis Experimental; Modelos Numéricos; Cercha de Viga de Piso.

1. Introduction

The dry construction system Light Steel Framing (LSF) represents a relevant alternative to conventional Brazilian building methods. This solution, composed mainly of cold-formed zinc-coated steel profiles and timber-based panels, enables faster construction, reduced waste generation, and cleaner construction sites. Within this system, floor beams and structural panels play an important role in the

overall performance of lightweight buildings.

Despite the growing use of LSF in Brazil, there is still a lack of studies and design guidance addressing the structural behavior of some of its subcomponents as complete systems. This gap is particularly evident in the case of floor members, which may be composed of single-section joists or trusses and may support either dry or wet floor decks.

Previous studies have investigated cold-formed steel floor systems from different perspectives, including composite interaction with concrete and timber decks (Güldür; Baran; Topkaya, 2021; Kyvelou; Gardner; Nethercot, 2018; Lakkavalli; Liu, 2006), dynamic performance (Xu; Tangorra, 2007), fire behavior (Hisham et al., 2025), the influence of connections on truss response (Dizdar; Baran; Topkaya, 2019; Ranasinghe et al., 2025; Țăranu; Toma, 2021), and the shear behavior of floor diaphragms (Baldassino; Zandonini; Zordan, 2021).

The available literature includes both numerical and experimental analyses of single-section cold-formed steel floor beams (Hisham et al., 2025; Kyvelou; Gardner; Nethercot, 2018; Lakkavalli; Liu, 2006; Xu; Tangorra, 2007), trussed floor systems (Dizdar; Baran; Topkaya, 2019; Güldür; Baran; Topkaya, 2021; Ranasinghe et al., 2025; Țăranu; Toma, 2021), and diaphragm-type floor assemblies (Baldassino; Zandonini; Zordan, 2021). Regarding deck materials, the reported studies include concrete decks (Baldassino; Zandonini; Zordan, 2021; Güldür; Baran; Topkaya, 2021; Lakkavalli; Liu, 2006), steel decks (Baldassino; Zandonini; Zordan, 2021), timber panels (Hisham et al., 2025; Kyvelou; Gardner; Nethercot, 2018; Țăranu; Toma, 2021; Xu; Tangorra, 2007), fibrocement boards (Hisham et al., 2025; Ranasinghe et al., 2025), and gypsum-fibre boards (Baldassino; Zandonini; Zordan, 2021).

Lakkavalli and Liu (2006) experimentally investigated different shear-transfer mechanisms in composite cold-formed steel C-section floor joists with concrete slabs. Kyvelou, Gardner and Nethercot (2018) employed finite element models to evaluate the flexural stiffness and strength of composite systems formed by cold-formed steel beams and OSB panels. Güldür, Baran and Topkaya (2021) studied cold-formed steel truss floors with concrete-filled compression chords by means of

full-scale tests and numerical modeling. Xu and Tangorra (2007) investigated the static and dynamic response of lightweight residential floors supported by cold-formed steel joists and OSB panels. More recently, Hisham et al. (2025) examined the behavior of LSF floors under fire and static loading, while Dizdar, Baran and Topkaya (2019), Țăranu and Toma (2021), and Ranasinghe et al. (2025) explored connection effects, instability, and failure modes in trussed cold-formed steel floor systems.

Although the literature is broad and current, some relevant gaps remain. First, most experimental studies on trussed floor systems are based on four-point bending arrangements, which are more closely associated with flexural strength assessment than with serviceability under realistic uniformly distributed floor loading. Second, only a limited number of studies address cold-formed steel floor trusses used together with OSB decking, and even fewer combine experimental investigation with a direct comparison among simplified numerical idealizations focused on service deflection. Third, the practical implications of different geometric idealizations for routine simulation of such systems remain insufficiently discussed.

In this context, the contribution of the present study can be understood at three levels. Methodologically, it uses a water-based loading system to reproduce a uniformly distributed service load. Experimentally, it evaluates a full-scale LSF floor subsystem composed of trusses and OSB decking. Practically, it compares three numerical idealizations and identifies the one that showed the best agreement with the measured service deflection. Accordingly, the objective of this study is to improve the understanding of the global service response of LSF floor trusses subjected to uniformly distributed loading by combining experimental testing and numerical simulation, taking the maximum vertical deflection measured at the midspan of the central truss as the primary response parameter for experimental–numerical comparison.

2. Prototype Specifications

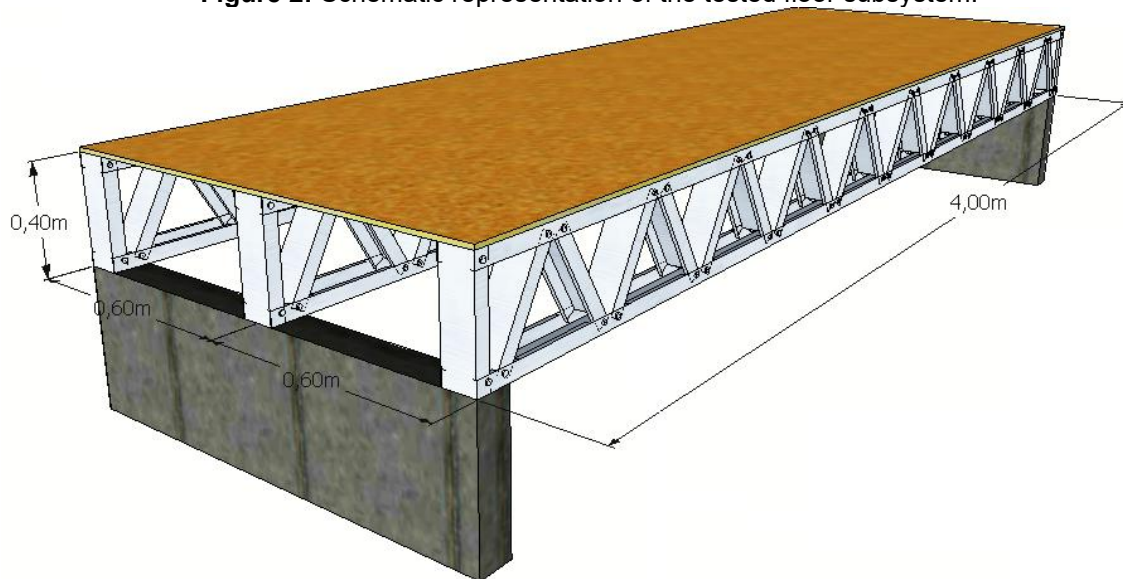
As illustrated in Figure 1, the tested floor subsystem consisted of three identical LSF beam trusses arranged side by side, each with a span of 4000 mm. The trusses were manufactured from Ue 89 x 41.3 x 10 x 0.95 mm ASTM A36 steel profiles with Z275 coating and connected by rivets. The total truss height was 400 mm, and the center-to-center spacing between adjacent trusses was 600 mm. OSB panels with thickness 18.3 mm were fixed to the top chords by hexagonal self-drilling screws, forming the floor surface used in the experiments.

Figure 1: Beam truss used in the experimental program.



Figure 2 presents the overall configuration of the tested floor subsystem, which represented a dry floor arrangement commonly employed in LSF buildings. The bottom and top chords were connected to the web members through riveted joints, with web elements forming approximately 60° with the horizontal axis. The OSB panels were included in the experimental assembly because they are frequently used in LSF floors due to their mechanical resistance and diaphragm action. However, the present study focuses on the global service response of the steel truss subsystem rather than on a detailed evaluation of panel–steel composite action.

Figure 2: Schematic representation of the tested floor subsystem.



According to AISI S214-12 (American Iron and Steel Institute, 2012), cold-formed steel truss systems shall be designed to safely resist the actions expected during their service life. In addition, ABNT NBR 6120 (Associação Brasileira de Normas Técnicas, 2019) establishes minimum vertical live loads for residential and office floors. In the present study, a uniformly distributed load of 3.0 kN/m^2 was adopted as the investigated service loading level. The experimental and numerical analyses focused on the vertical displacement of the central truss under this loading condition.

3. Laboratory Experimental Tests

The laboratory tests were designed to measure the vertical displacement of the LSF floor truss subsystem under a uniformly distributed load. To reproduce this loading condition, a water tank was built on top of the floor assembly and gradually filled during the tests.

A water column was adopted because water naturally maintains a level surface and allows direct control of the applied pressure through the measured water height. At room temperature, water has a specific weight of approximately 9.81 kN/m^3 . Accordingly, each 1 cm increase in water height corresponds to an

increase of about 0.1 kN/m^2 in the distributed surface load.

The tank was built with MDF boards and had a total self-weight of 91.08 kg. A plastic tarp was used to prevent leakage during the tests. All experimental procedures were carried out at the Laboratório de Ensaios em Sistemas Estruturais (LESE) of the University of Passo Fundo.

Figure 3 shows the complete laboratory setup adopted in the tests. During the experimental program, the tank was slowly filled with water by means of a hose and a flow meter, and the applied loading was controlled by monitoring both the water height and the water volume. The vertical displacement was measured only at the midspan of the central truss by means of a digital gauge with millimetric readings and thousandth precision. The loading was applied in increments corresponding to 5 cm of water height, that is, 0.5 kN/m^2 , until the investigated service load of 3.0 kN/m^2 was reached.

Figure 3: Experimental setup used in the laboratory tests.



It should be emphasized that the repeated tests reported in this study were performed on the same full-scale experimental assembly, rather than on independent specimens. Accordingly, the experimental program does not provide a

statistical assessment of specimen-to-specimen variability, which should be recognized as a limitation of the study. Since the applied loading was restricted to the service range considered herein and no permanent damage was observed during testing, reusing the same prototype was considered acceptable for the specific purpose of comparing the measured service deflections with the numerical results. Therefore, the repeated tests should be interpreted as repeated measurements on a single structural system under similar loading conditions, and not as evidence of experimental variability between independent prototypes.

4. Computer Simulations FEM Analysis

Three numerical models were developed based on the dimensions and geometry of the tested truss system. The investigated models were: (i) a three-dimensional shell model with web-connection eccentricity; (ii) a two-dimensional beam model with web-connection eccentricity; and (iii) a two-dimensional beam model without web-connection eccentricity. All simulations were performed in ANSYS Workbench by linear static analysis, consistently with the objective of reproducing the global service response of the tested system under the investigated loading range.

4.1 Material Properties

The steel members were modeled as linear-elastic, isotropic material. The adopted mechanical properties were a modulus of elasticity $E = 200$ GPa and a Poisson's ratio $\nu = 0.30$. The nominal thickness of the cold-formed steel profiles used in the experimental prototype and in the numerical models was 0.95 mm.

Linear static analysis was adopted because the purpose of the study was to compare the global serviceability response of the floor truss system under a uniformly distributed service load, taking the measured vertical deflection as the main response parameter. Therefore, geometric and material nonlinearities, initial imperfections, and local failure mechanisms were not considered in the present

models.

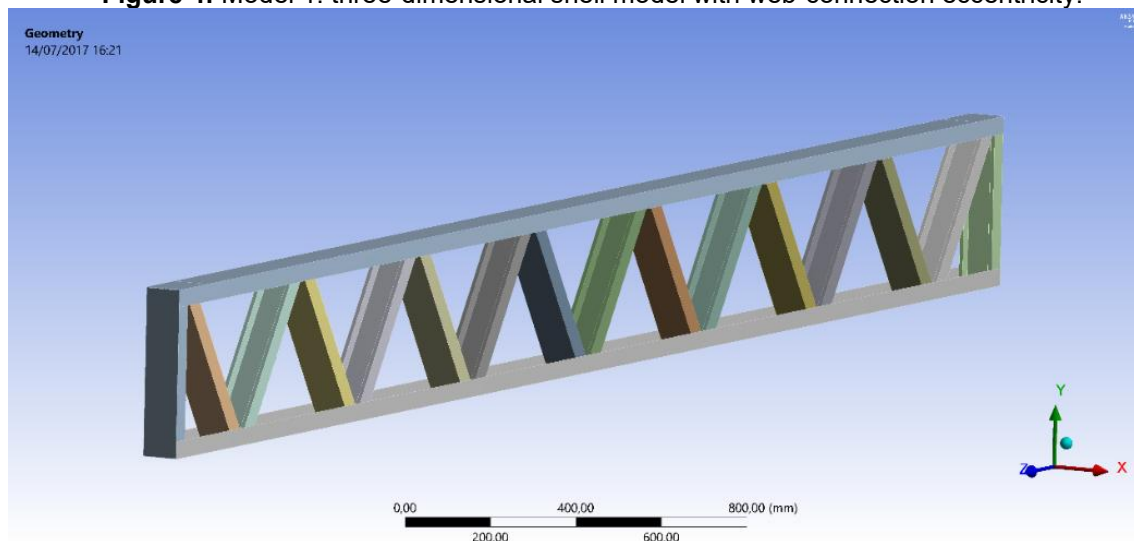
The actual truss was assembled by riveted connections. In the numerical simulations, these joints were represented by simplified contact or connectivity assumptions consistent with each model idealization. This simplification is acceptable for comparing global service deflections, but it is not intended to reproduce local stress concentrations, connection slip, or joint failure phenomena.

The OSB panels were not explicitly modeled as structural elements with detailed panel–steel interaction, screw behavior, or relative slip. Their participation was considered only through the applied loading condition. Consequently, the numerical models should be interpreted as simplified tools for predicting the global service deflection of the truss system, rather than as detailed representations of composite action between the trusses and the OSB panels.

4.2 Tridimensional Shell with Eccentricity Model

In Model 1, whose geometry is illustrated in Figure 4, the truss was represented in three dimensions and the steel members were modeled as thin shells. The eccentricity between the web members and the top and bottom chords was explicitly included.

Figure 4: Model 1: three-dimensional shell model with web-connection eccentricity.



The finite element mesh was generated with SHELL181 elements, with a maximum element size of 10 mm. The model contained 28,704 nodes and 15,624 contact elements (CONTA174, TARGE170, and SURF154), totaling 42,478 elements. The support conditions reproduced the laboratory setup, with one end restrained in the x, y, and z directions and the opposite end restrained in the y and z directions over the corresponding support region.

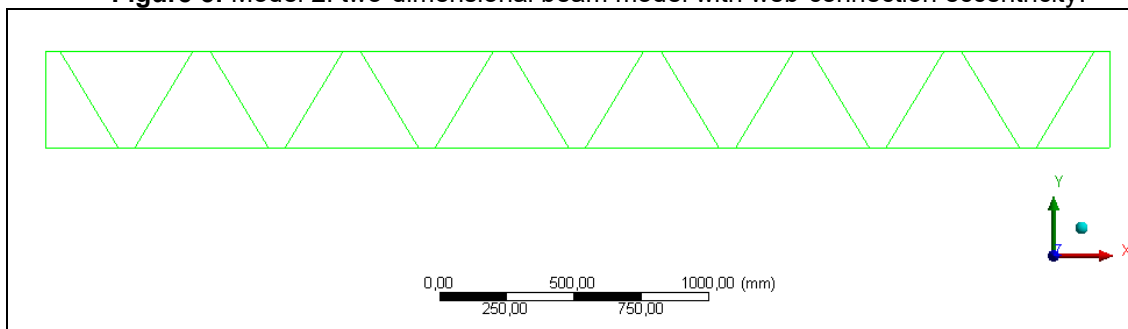
The loading adopted in the experiment was a uniformly distributed surface load of 3.0 kN/m² acting on the floor subsystem. For interpretation at the level of the central truss, this corresponds to a tributary line load of 1.80 kN/m, obtained from the tributary width associated with the truss spacing (3.0 kN/m² × 0.60 m). In the three-dimensional shell model, the same resultant action was represented as an equivalent pressure distributed over the loaded area of the top chord, so that the total load remained consistent with the tributary action derived from the experimental arrangement. In addition, the self-weight contribution of the water tank was included as an equivalent distributed action.

After the geometry, material properties, boundary conditions, and loading were defined, the deformation of the shell model was obtained by linear static analysis. It should be noted that this model was intended to reproduce the global elastic response of the tested system and not local nonlinear effects in the connections.

4.3 Bidimensional Beam with Eccentricity Model

For Model 2, shown in Figure 5, a two-dimensional beam idealization was adopted while maintaining the same material properties, support conditions, and load combinations used in the previous model. In this case, the eccentricity of the web connections with respect to the top and bottom chords was explicitly represented in the beam formulation.

Figure 5: Model 2: two-dimensional beam model with web-connection eccentricity.

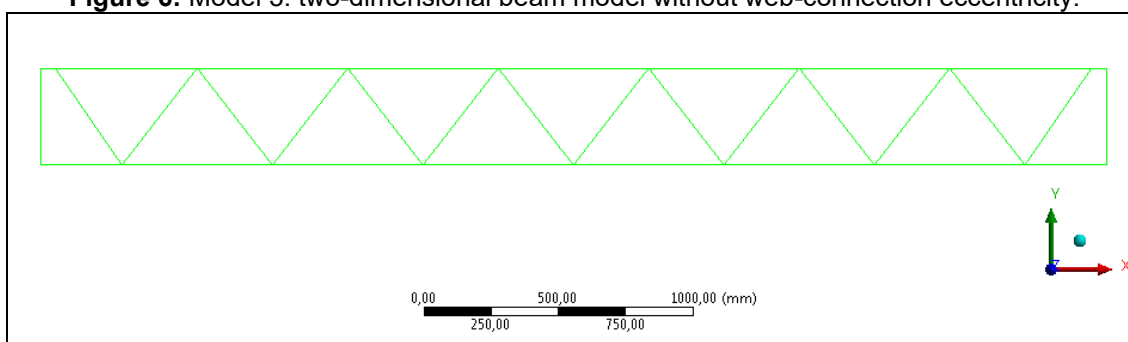


The finite element mesh was generated with BEAM188 elements. The resulting model contained 2,926 nodes, 786 contact elements (SURF156), and 2,256 elements in total. Linear static analysis was again adopted, since the focus remained on the measured service deflection of the central truss.

4.4 Bidimensional Beam Without Eccentricity Model

Model 3, presented in Figure 6, was also developed as a two-dimensional beam idealization, but without explicit representation of the eccentricity between the web members and the chords. The same material properties, loading conditions, and support conditions adopted in the previous models were maintained.

Figure 6: Model 3: two-dimensional beam model without web-connection eccentricity.



The finite element mesh was generated with BEAM188 elements and resulted in 3,004 nodes, 774 contact elements (SURF156), and 2,283 elements. As in the previous cases, the analysis was restricted to linear static response

under the investigated service loading.

5. Results Analysis

The experimental and numerical results were compared on the basis of the maximum vertical displacement measured at the midspan of the central truss. As summarized in Table 1, three repeated tests were carried out with the same full-scale floor assembly, and the displacement values measured at the investigated load level of 3.0 kN/m² are reported for each repetition.

Table 1: Experimental results for the repeated tests.

Test	Measured deflection at 3.0 kN/m ² (mm)
Test 1	4.29
Test 2	4.16
Test 3	4.08
Average	4.18

The measured deflections for the repeated tests were 4.29 mm, 4.16 mm, and 4.08 mm, resulting in an average value of 4.18 mm. A slight decrease in the measured displacement was observed from the first to the third test. Since the same experimental assembly was reused, this trend is interpreted as possible initial accommodation of the system, including seating at supports, local adjustment of mechanical connections, and minor rearrangement of contacts between components. For this reason, the repeated tests should not be interpreted as evidence of statistical repeatability, but rather as repeated measurements on the same structural system under similar service-loading conditions.

The expected linear-elastic response was observed throughout the investigated loading range. According to ABNT NBR 14762 (Associação Brasileira de Normas Técnicas, 2010), the serviceability limit for the deflection of simply supported floor beams may be expressed as $\delta = L/350$. For the 4000 mm span considered in the present study, this limit corresponds to 11.43 mm. Therefore, the measured deflections remained below the adopted serviceability limit for the investigated loading level. This normative verification is restricted to serviceability performance in terms of vertical displacement and does not imply assessment of

ultimate strength, buckling resistance, connection durability, or dynamic performance.

The numerical results are discussed below with reference to the displacement fields obtained for each model. Figures 7, 8, and 9 present the response patterns for Models 1, 2, and 3, respectively, while Table 2 summarizes the corresponding maximum deflections and divergences relative to the experimental average.

Figure 7: Displacement field obtained for Model 1.

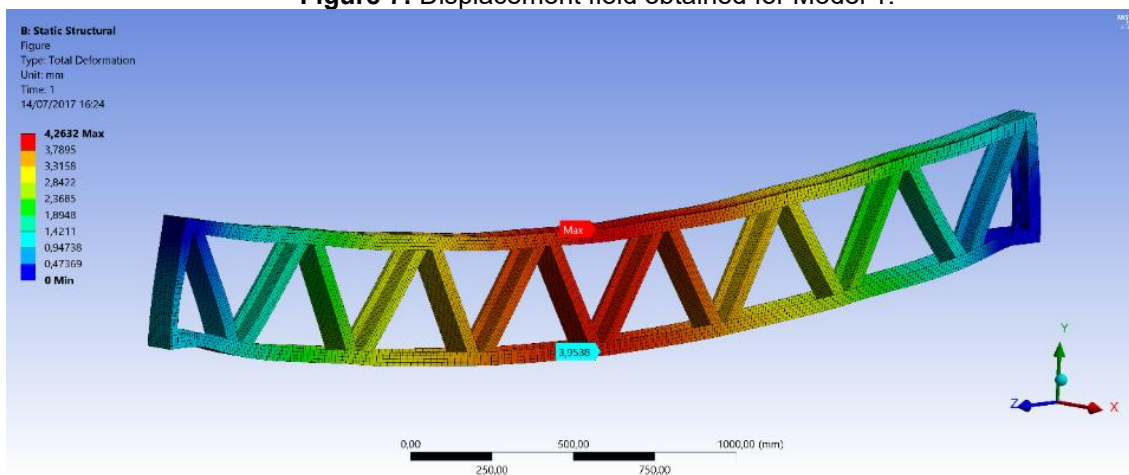


Figure 8: Displacement field obtained for Model 2.

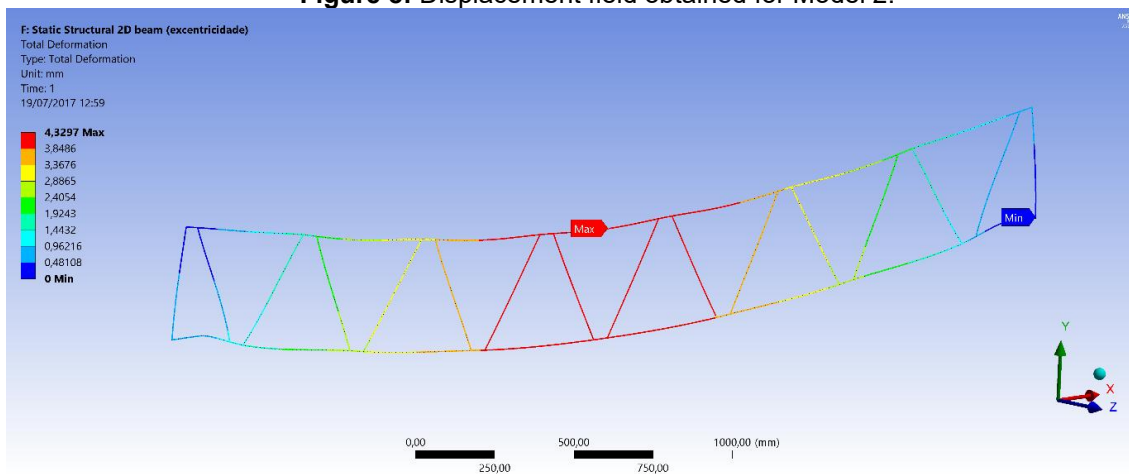


Figure 9: Displacement field obtained for Model 3.

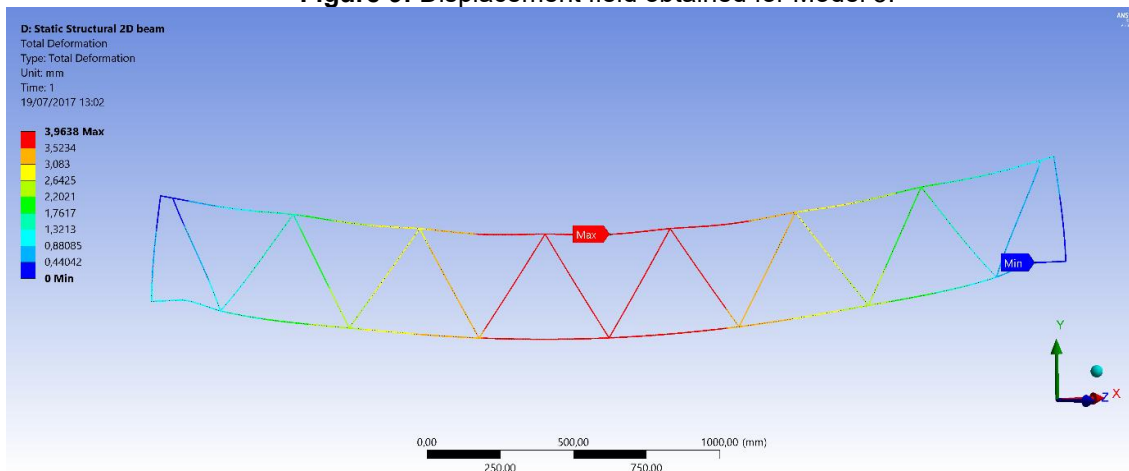


Table 2: Numerical displacement results and divergence relative to the experimental average.

Model	Displacement (mm)	Divergence
Model 1	3.96	5.19%
Model 2	4.27	2.23%
Model 3	3.92	6.15%

The comparison shows that the explicit consideration of web-connection eccentricity is relevant for reproducing the measured service deflection. The two-dimensional beam model with eccentricity provided the closest agreement with the experimental value, whereas the shell model with eccentricity and the two-dimensional beam model without eccentricity underestimated the measured displacement. Based on the response parameter adopted in this study, Model 2 showed the best agreement with the measured service deflection of the central truss.

This agreement, however, should be interpreted with caution. The comparison performed herein is restricted to a single response parameter, namely the maximum vertical deflection measured at midspan under a specific service-loading condition. Therefore, the results do not constitute a comprehensive validation of the numerical model for all aspects of structural behavior, such as local stresses, rotational response, connection behavior, or failure mechanisms.

6. Conclusions

For the tested configuration and for the service loading level considered in this study, the measured vertical displacements remained below the adopted serviceability limit. Therefore, the experimental results indicate adequate serviceability performance of the investigated LSF floor subsystem under the evaluated loading condition.

Regarding the numerical analyses, all investigated models produced deflections with divergence lower than 10% relative to the experimental average. Among them, the two-dimensional beam model with explicit web-connection eccentricity showed the best agreement with the measured service deflection, with a divergence of 2.23%. Accordingly, among the investigated idealizations, this model is the most suitable for simplified serviceability-oriented simulations of similar LSF floor beam trusses.

The conclusions of the present study are restricted to the global service response represented by the measured vertical deflection of the central truss. No claim is made regarding ultimate capacity, collapse resistance, or failure margins, since such assessment would require specific investigation of nonlinear behavior, instability phenomena, and connection failure modes.

Finally, the study also has important limitations that should be acknowledged. The repeated tests were carried out on the same full-scale experimental assembly, the numerical comparison was based on a single measured response quantity, and the OSB panels were not explicitly modeled as structural components in the numerical simulations. Future studies should include independent specimens, additional experimental response parameters, and more detailed numerical representation of connection flexibility and panel–steel interaction.

References

AMERICAN IRON AND STEEL INSTITUTE. AISI S214-12: *North American standard for cold-formed steel framing — truss design*. Washington, DC: AISI, 2012.

ASSOCIAÇÃO BRASILEIRA DE NORMAS TÉCNICAS. NBR 6120: *cargas para o cálculo de estruturas de edificações*. Rio de Janeiro: ABNT, 2019.

ASSOCIAÇÃO BRASILEIRA DE NORMAS TÉCNICAS. NBR 14762: *dimensionamento de estruturas de aço constituídas por perfis formados a frio*. Rio de Janeiro: ABNT, 2010.

BALDASSINO, N.; ZANDONINI, R.; ZORDAN, M. Experimental study of the shear behaviour of floor diaphragms in light steel residential buildings. *Thin-Walled Structures*, v. 167, p. 108099, 2021. DOI: 10.1016/j.tws.2021.108099.

DIZDAR, Ç.; BARAN, E.; TOPKAYA, C. Strength and stiffness of floor trusses fabricated from cold formed steel lipped channels. *Engineering Structures*, v. 181, p. 437-457, 2019. DOI: 10.1016/j.engstruct.2018.12.041.

EUROPEAN COMMITTEE FOR STANDARDIZATION. EN 300:2006: *oriented strand boards (OSB) — definitions, classification and specifications*. Brussels: European Committee for Standardization, 2006.

GÜLDÜR, H.; BARAN, E.; TOPKAYA, C. Experimental and numerical analysis of cold formed steel floor trusses with concrete filled compression chord. *Engineering Structures*, v. 234, p. 111813, 2021. DOI: 10.1016/j.engstruct.2020.111813.

HISHAM, F.; MAHENDRAN, M.; VY, S. T.; ARIYANAYAGAM, A. Numerical modelling of light gauge steel framed floors under standard fire conditions. *Journal of Constructional Steel Research*, v. 233, p. 109626, 2025. DOI: 10.1016/j.jcsr.2025.109626.

KYVELOU, P.; GARDNER, L.; NETHERCOT, D. A. Finite element modelling of composite cold-formed steel flooring systems. *Engineering Structures*, v. 158, p. 28-

42, 2018. DOI: 10.1016/j.engstruct.2017.12.024.

LAKKAVALLI, B. S.; LIU, Y. Experimental study of composite cold formed steel C section floor joists. *Journal of Constructional Steel Research*, v. 62, p. 995-1006, 2006. DOI: 10.1016/j.jcsr.2006.02.003.

RANASINGHE, G.; VY, S. T.; MAHENDRAN, M.; ARIYANAYAGAM, A.
Experimental study of LSF truss floor ceiling systems made of top hat sections. *Thin-Walled Structures*, v. 212, p. 113193, 2025. DOI: 10.1016/j.tws.2025.113193.

ȚĂRANU, G.; TOMA, I.-O. FEM analysis of a floor structural system made of thin walled cold formed steel profiles. *IOP Conference Series: Materials Science and Engineering*, v. 1141, p. 012033, 2021. DOI: 10.1088/1757-899X/1141/1/012033.

XU, L.; TANGORRA, F. M. Experimental investigation of lightweight residential floors supported by cold formed steel C shape joists. *Journal of Constructional Steel Research*, v. 63, p. 422-435, 2007. DOI: 10.1016/j.jcsr.2006.05.010.